ELSEVIER

Dyes and Pigments 40 (1999) 251–259

DYES AND PIGMENTS

Dicyanopyrazine studies. Part VII: Solid state absorption spectra and aggregation behavior of aminovinylpyrazine dyes containing a long chain alkyl group

Jae-yun Jaung[a], Masaru Matsuoka[b,*], Koushi Fukunishia[a]

[a]*Department of Chemistry and Materials Technology, Kyoto Institute of Technology, Matsugasaki, Sakyo-ku, Kyoto 606-0962, Japan*
[b]*Laboratory of Material Science, Kyoto Women's University, Imakumano, Higashiyama-ku, Kyoto 605-8501, Japan*

Received 1 July 1998; accepted 27 July 1998

Abstract

The solid state absorption maxima of aminovinylpyrazine dyes containing long chain alkyl groups were changed drastically by the differences in their molecular stacking. The spectral shift from solution to the solid state was evaluated by the $\Delta\lambda$ values, and the shift was correlated with substituent effects and their three dimensional molecular structures. Related dyes were synthesized by the nucleophilic substitution of 2,3-dichloro-5,6-dicyanopyrazine with various Fisher's base type enamines having long alkyl chain groups. © 1998 Elsevier Science Ltd. All rights reserved.

Keywords: Aminovinylpyrazine; Intermolecular $\pi - \pi$ interaction; Molecular stacking; Solid state spectra; Fluorescence dye

1. Introduction

The absorption and emission spectra of dyes are strongly affected by their aggregation behavior. Cyanine dyes are known to exist as equilibrium mixtures of monomer, dimer and aggregates in solution. The J-aggregate shows distinct spectral changes in λ max and band shape compared to those of the corresponding monomer. The relationship between the molecular arrangements and the spectral shifts of dye aggregates has been explained in terms of the molecular exciton theory [1]. McRae and Kasha [2] suggested that a lateral displacement of adjacent dye molecules to form a parallel pair shifts a monomer absorption band to longer wavelength and produces the J-band, while a pairwise stacking to cancel their dipole moment causes a hypsochromic shift of λ max and produces the H-band. The band shape of the J-band is very sharp having intensive absorption which was rationalized by Briggs and Herzenberg [3] by the coherent exciton scattering method. It has been suggested that the band will be sharp when the exciton interaction is much stronger than the coupling of the molecular vibration.

We intend to design new types of aminovinylpyrazine dyes having the ability to produce intermolecular $\pi - \pi$ interactions. In this paper, aminovinylpyrazine dyes with long chain alkyl groups were synthesized and their spectral properties evaluated in the solid state and correlated with their molecular stacking.

* Corresponding author. Tel.: +81-75-531-7175; fax: +81-75-531-7175-; e-mail: gha14151@nifty.ne.jp

0143-7208/98/$—see front matter
PII: S0143-7208(98)00065-5

2. Results and discussion

2.1. Syntheses of aminovinyl pyrazine dyes

The reaction of 2,3-dichloro-5,6-dicyanopyrazine **2** with Fisher's type base to give aminovinylpyrazine fluorescence dyes has been reported in our previous paper [4]. 2-Chloro-5,6-dicyano-3-[2′-(1′-N-alkyl-3′,3′-dimethylindolinylidene)methyl]-pyrazines (**3a**∼**3d**) were synthesized in 55∼97% yields by the reaction of **2** with 2 equiv. of 1-alkyl-3,3-dimethyl-2-methyleneindoline **1**, which in turn was previously obtained from 2,3,3-trimethylindolenine with an alkyl bromide in the presence of sodium hydroxide (Scheme 1). 1-*N*-Alkyl-2-methylenequinoline and 1-*N*-alkyl-4-methylenequinoline were synthesized by similar reactions of 2- and 4-methylquinoline with alkylbromides, respectively. These enamines gave the corresponding aminovinylpyrazines **4** and **5**, in moderate yields. Further reactions of **3** or **5** with 2 equiv. of 1,2-bis(2-aminoethoxy)ethane in the presence of

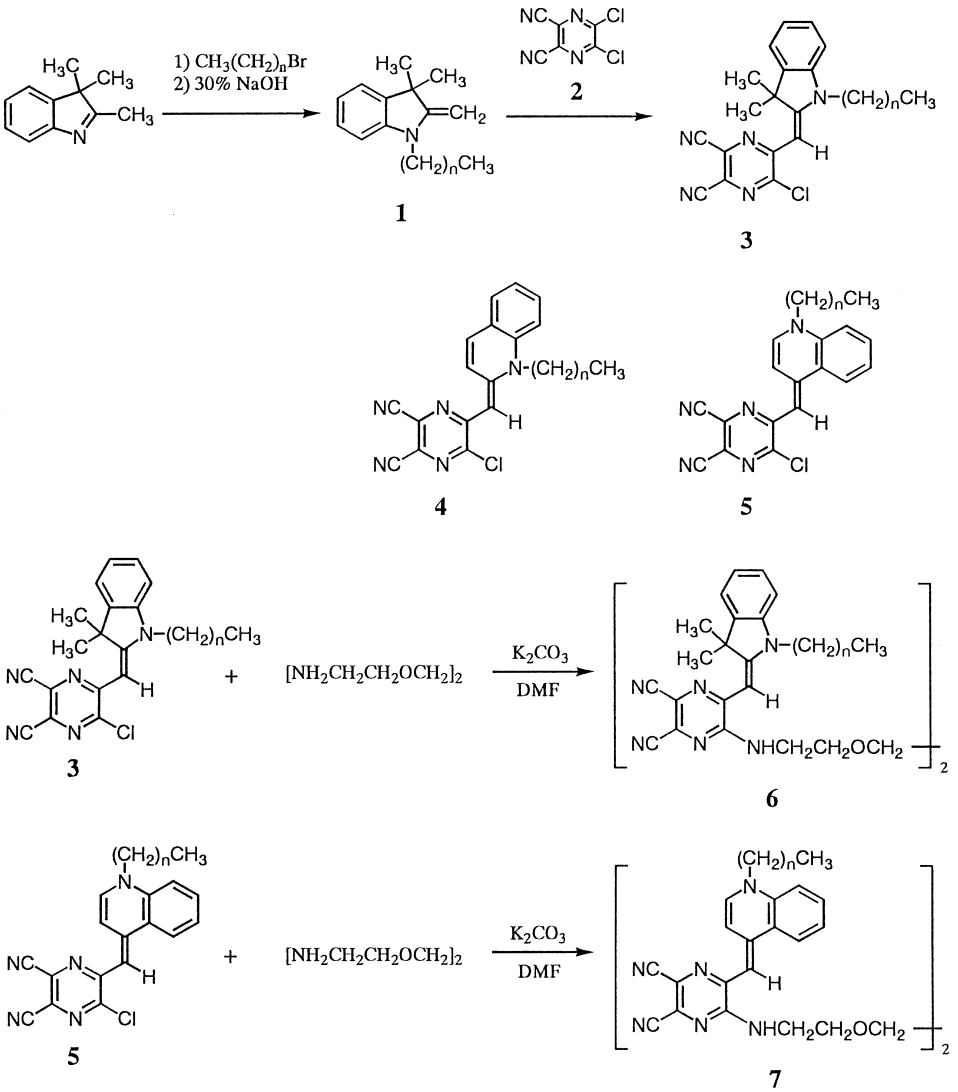

Scheme 1.

potassium carbonate in *N*,*N*-dimethylformamide gave the corresponding bisaminovinylpyrazines **6** or **7** in good yields.

The ^{1}H NMR spectra showed that the olefinic proton of **5** was apparent at much more downfield, around 0.8 ppm, than those of **3** and **4**, which might be caused by the additional ring current effect from the quinoline ring (Table 1).

Similarly, the olefinic proton of **7** was observed at 6.18 ppm, while that of **6** was observed at around 5.4 ppm. The upper field shift of the olefinic proton from the monomeric dyes (**3** and **5**) to the dimeric dyes (**6** and **7**) was caused to the electron donating property of the alkylamino group at the 2-position replacing the chlorine atom.

Some dyes have a wide melting point range, which is caused by their liquid crystal behavior based on their long chain alkyl group. Similar dyes with shorter chain alkyl groups (**3a** and **4a**) have narrow melting ranges. Dyes **5b** and **5c** have a large dipole moment and the presence of a long chain alkyl group did not results in a wide melting point range. Dyes **6** and **7** also did not show a wide melting point range, which results from the restriction of molecular mobility by the introduction of the crosslinking moiety. From these results, it was concluded that dyes **5** have strong intermolecular $\pi-\pi$ interactions, which cancel their dipole moment in the molecular pair.

Table 1
Aminovinylpyrazines derivatives **3–7**

Compd.	*n*	mp(°C)	mz[a]	^{1}H NMR (δ Ha[b], ppm)
3a	0	272∼273	1	5.91[c]
3b	8	92∼106	14[d]	5.98[c]
3c	10	95∼101	6	5.98[c]
3d	15	262∼270	8	5.90
4a	0	298∼300	2	5.99[c]
4b	8	150∼164	14	6.00[c]
5a	3	250∼251	1	6.85[c]
5b	8	164∼169	5	6.76[c]
5c	15	148∼152	4	6.81[c]
6a	0	221∼225	4	5.37[e]
6b	10	117∼118	1	547[e], 5.55
7	15	112∼114	2	6.18[e]

[a]Melting zone.
[b]Methine proton.
[c]In $CDCl_3$.
[d]103 and 113°C by DSC.
[e]In DMSO-d_6.

The ^{1}H NMR spectra of **3a** and **6a** are shown in Fig. 1. The signals for H^a, H^b and N-CH_3 of **3a** appear as singlets at 5.91, 3.42 and 1.61 ppm, respectively. On the other hand, dye **6a** showed two sets of signals; H^b (1.62 and 1.37 ppm), N-CH_3 (3.33 and 3.11 ppm), NH (8.07 and 7.92 ppm), H^a (5.37 and 5.35 ppm), respectively; all methylene protons in **6a** were observed at around 3.51∼3.60 ppm.

This splitting of the chemical shifts for each proton was caused by the restriction of rotation between the two pyrazine chromophores through the crosslinked unit. As a result, **6a** exists as two stable conformers in the ratio of 5:2 in DMSO-d_6 at room temperature.

Temperature dependence ^{1}H NMR spectra of **6b** are shown in Fig. 2. Dye **6b** showed two sets of

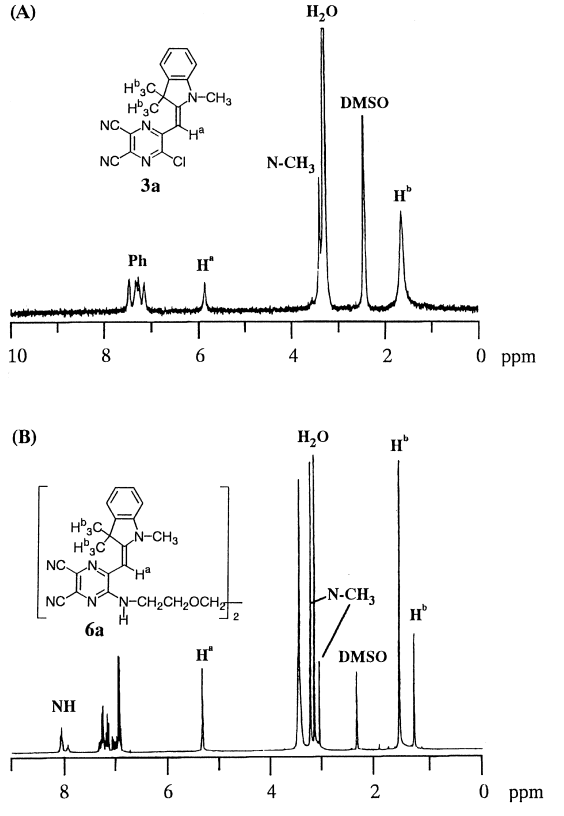

Fig. 1. 300 MHz ^{1}H NMR spectra of **3a** (A) and **6a** (B) in DMSO-d_6.

signals at 22°C, but these splittings almost disappeared at 80°C. These results indicate the increase of molecular rotation at higher temperature, and consequently the full rotation of the two chromophoric moieties was restricted at lower temperature.

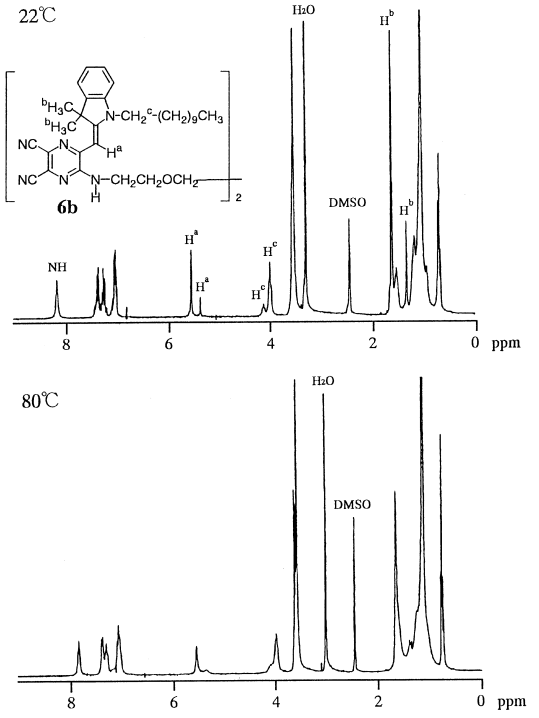

Fig. 2. Temperature dependence ^{1}H NMR spectra of **6b** in DMSO-d_6.

2.2. Absorption and fluorescence spectra in solution and the solid state

The PPP MO calculation results revealed that the basic chromophore of **3** and **5** has a strong intramolecular charge-transfer chromophoric system in which the dicyanopyrazine moiety acts as an acceptor and the aminovinyl moiety acts as a donor. The π-electron density changes accompanying the first excitation are shown in Fig. 3.

In a previous paper [4], the optimized molecular structures of the parent chromophores of **3**, **4** and **5** were evaluated by using the MOPAC PM 3 method. Dye **3** has a twisted structure between the two π-ring systems and the dihedral angle was calculated as 40°. The bent structure was caused by the steric hindrances between the *N*-methyl or the isopropyl groups and the lone pair electron of the pyrazine ring. The optimized structures for dyes **4** and **5** have planar π-conjugated system, and dye **5** has the largest ε value compared with those of **3** and **4** which is caused by the most effective π-conjugation without any steric hindrances [4]. The dipole moments in the ground state of the *N*-methyl derivatives of these dyes were calculated by the PPP MO method, and these were 9.638 debye for **3**, 11.215 for **4** and 11.687 for **5**.

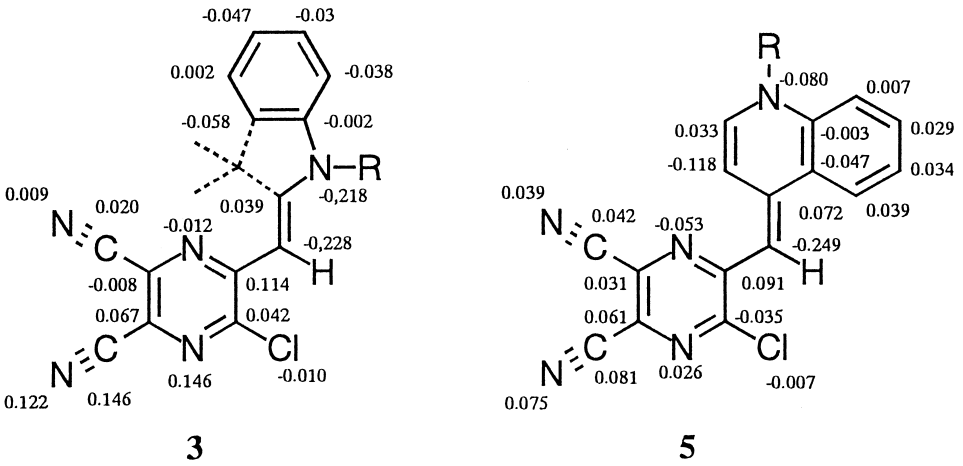

Fig. 3. π-Electron density changes accompanying the first excitation of **3** and **5** by the PPP MO method.

Dye **5** has the largest dipole moment of the above dyes, and has a completely planar structure. As a result, intermolecular electrostatic interactions to cancel the dipole moment will compete with the intermolecular hydrophobic interactions of the long chain alkyl groups to arrange the molecule in the same direction. These intermolecular interactions influence their absorption and fluorescence spectra in the solid state.

Table 2 shows the visible and fluorescence spectra of dyes **3**–**7** in solution and in the solid state. The absorption maxima of these dyes in solution were observed at around 465∼560 nm while those in the solid state were observed at around 467∼619 nm. Dyes **3a**–**3d** absorbed at around 472 nm in chloroform but the λ max values of these dyes in the solid state changed significantly with differences in chain length of the alkyl group, viz., from 487 nm to 585 nm.

The effect of molecular aggregation on the absorption spectra were evaluated by the $\Delta\lambda$ values. Dye **3a** has a large $\Delta\lambda$ value of 113 nm, which indicates strong intermolecular $\pi-\pi$ interactions in the solid state. Dye **3b** ($n=8$) and **3c** ($n=10$) showed relatively small $\Delta\lambda$ values compared with **3a** ($n=0$). The $\Delta\lambda$ values increased in accord with the chain length of the N-alkyl group.

Time dependence absorption spectra of **3b** ($n=8$) in vapor deposited thin film are shown in Fig. 4. The spectra changed gradually, depending on the time after preparation of the film, and new absorption maxima were observed at 540 nm and 560 nm. These results indicate that molecular stacking proceeded step by step by intermolecular interactions such as the hydrophobic interactions of the long chain alkyl group.

Dye **4b** showed positive $\Delta\lambda$ values while **4a** showed negative $\Delta\lambda$ values. These differences in $\Delta\lambda$ values depended on the chain length of the alkyl group and can be explained in terms of differences in molecular stacking in the solid state; dye **4** has large dipole moment of 11.2 debye in the ground state, and a head-to-tail molecular arrangement to cancel the dipole moment will occur in the case of **4a**, but hydrophobic interactions of the long chain alkyl group to promote the

Table 2
Visible and fluorescence spectra of dyes **3**–**9**

Compd.	n	λ ma (nm)		$\Delta\lambda$[b] (nm)	Fmax (nm)		ΔF[e] (nm)	SS[f] (nm)
		$CHCl_1$	Solid[a]		$CHCl_3$[c]	Solid[d]		
3a	0	472	585	113	540	625	85	68
3b	8	471	487	16	550	597	47	79
3c	10	471	518	47	556	610	54	85
3d	15	473	561	88	558	627	69	85
4a	0	536	515	–21	–	–	–	–
4b	8	531	582	51	–	–	–	–
5a	3	560	619	59	–	–	–	–
5b	8	552	474	–78	–	–	–	–
5c	15	552	467	15	–	–	–	–
6a	0	465	483	18	513	559	46	48
6b	10	471	563	92	510	622	112	39
7	15	518	510		–	–	–	–
		570[g]	575	57				

[a]Vapor deposited thin film
[b]$\Delta\lambda = \lambda$ max (solid)–λ max ($CHCl_3$).
[c]Fluorescence maximum excited at λ max value.
[d]Solid state fluorescence maximum excited at 360 nm.
[e]$\Delta F = F$ max (solid)–F max (soln.).
[f]Stokes shift.
[g]Shoulder

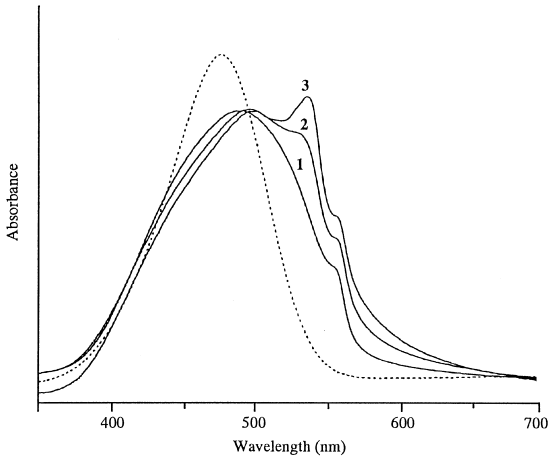

Fig. 4. Time dependence absorption spectra of **3b** in the vapor deposited thin film: 1(0.1 h), 2(3 h), 3(24 h), (- - - -) in chloroform.

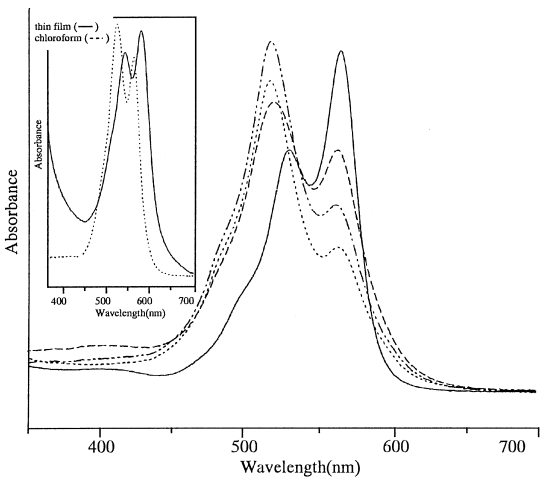

Fig. 5. The effect of solvent polarities on the absorption spectra of dye **7**; dimethylformamide (—), ethanol (– –), chloroform (– - - –), benzene (- - - -).

head-to-head arrangement will become predominant for **4b**.

On the other hand, the reverse situation was observed in the case of dyes **5**. Dye **5** has a much larger dipole moment of 11.7 debye in the straight direction from donor to acceptor, and the alkyl group is completely isolated from the pyrazine moiety.

As a result, cancellation of the large dipole moment will become predominant in comparison with the hydrophobic interactions of the alkyl group. It is generally observed that an alkyl group such as *n*-butyl tends to orient out of the π-plane in the molecular stacking of dye chromophores, because of strong intermolecular $\pi - \pi$ interactions [5,6].

The λ max of **6** in the solid state showed the same tendency as that of **3**, and $\Delta\lambda$ increases with the length of the *N*-alkyl group. Intra- and/or intermolecular interactions of the chromophores will be affected by the chain length of the alkyl groups and of the position of the substituent. Dyes **6** showed a single absorption maximum in the visible region, but dye **7** showed two absorption maxima around 510 and 570 nm. Their relative absorbances were affected largely by the solvent polarity; the absorbance at around 510 nm decreased with increase of solvent polarity and the reverse was observed for the longer wavelength absorption at around 570 nm (Fig. 5). The absorption spectra of dye **7** in an aprotic polar solvent (dimethyl sulfoxide) showed similar spectral curves to that of the vapor deposited thin film, indicating the similiarity of the intermolecular interactions of the chromophores.

2.3. Thermal property

Thermal properties of dye **3b** ($n = 8$) were evaluated by means of the TG (thermo-gravimetric) and DSC (differential scanning calorimetry) analyses (Fig. 6). It was observed that **3b** undergoes a reversible phase transfer arising from a reversible heat induced isomerisation. The DSC curve exhibited two endothermic peaks at 103 and 113°C without any weight loss.

The weight loss was observed at around 350°C, along with decomposition which started at 248°C. The weight loss (40%) was deduced to be due to the decomposition of the 1′-*n*-nonyl-3′,3′-dimethylindole moiety. These observations were common for the other derivatives of dye **3**, and dyes **3** with long chain alkyl group showed phase transfer and decomposed at around 250°C.

3. Experimental

Characterization of dyes were carried out by standard procedures using following equipment:

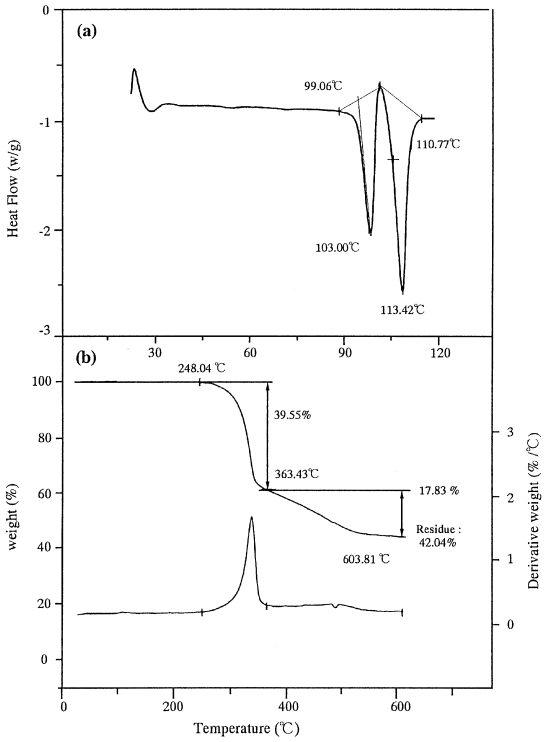

Fig. 6. Thermal properties of **3b** evaluated by DSC (a) and TGA (b).

melting points were determined on a Yanagimoto micro melting point apparatus without correction. The ^{1}H NMR spectra were taken on an FT-NMR QE 300 MHz Shimadzu spectrometer, and the ms spectra on an M-80 B Hitachi mass spectrometer. Visible and fluorescence spectra were measured on a U-3410 Hitachi spectrophotometer and a Shimadzu RF-5000 fluorescence spectrophotometer. Microanalysis was conducted with a Yanaco CHN MT-3 recorder. All chemicals were of reagent grade and were used without further purification, unless otherwise specified. Dyes **3a**, **4a** and **5a** have been previously reported [4].

*3.1. Syntheses of **3–5***

A solution of 2,3,3-trimethylindolenine (25 mmoles) and the appropriate *n*-alkyl bromide (50 mmoles) was refluxed for 10 h and cooled to room temperature. To the reaction mixture was added ethylacetate (10 ml), and the mixture was stirred at room temperature for 30 min. The precipitate was filtered, and washed with ether. The crude 1-alkyl-2,3,3-trimethylindolenine bromide was dissolved in chloroform (50 ml) and added to a mixture of water (40 g) and ice (40 g). To the reaction mixture was added dropwise 10 ml of 20% sodium hydroxide solution, and then the mixture was stirred for 30 min. The mixture was extracted with chloroform (2×40 ml) and dried over sodium sulfate. Evaporation of the extract gave the crude Fisher's base type enamine. To a solution of **2** (0.50 g, 2.5 mmoles) in tetrahydrofuran (15 ml) was added dropwise the crude enamine (5 mmoles), and the mixture was then stirred at room temperature for 2 h. The reaction mixture was poured into 70 ml of water. The precipitate was filtered, washed with water and dried. The compounds were recrystallized from benzene.

*3.1.1. 2-Chloro-5,6-dicyano-3-[2′-(1′*n*-nonyl-3′,3′-dimethylindolinylidene)methyl]pyrazine (**3b**)*

Red crystals (63% yield) ir: ν CN 2220 cm^{-1}; ms: m/z 449 ([M+2]$^+$), 447 (M$^+$); ^{1}H NMR ($CDCl_3$): δ 7.31–7.25 ((t+d), 2H, phenyl protons), 7.13 (t, 1H, J 7.2, phenyl proton), 6.90 (*d*, 1H, J 7.2, phenyl proton), 5.98 (s, 1H, –CH=), 3.84 (br. t, 2H, J 6.9, NCH_2), 1.79(br. s, 8H, $2CH_3$ and CH_2), 1.70–1.28 (m, 12H, CH_2), 0.88 (t, 3H, J 6.9, CH_3). Anal. Calcd. for $C_{26}H_{30}N_5Cl$: C, 69.71; H, 6.75; N, 15.63. Found: C, 69.11; H, 6.61; N, 15.78.

3.1.2. 2-Chloro-5,6-dicyano-3-[2′-(1′-n-*undecyl-3′,3′-dimethylindolinylidene)methyl]pyrazine (**3c**)*

Red crystals (55% yield) ir: ν CN2226 cm^{-1}; ms: m/z 477 ([M+2]$^+$), 475 (M$^+$); ^{1}H NMR ($CDCl_3$): δ 7.30–7.25 ((t+d), 2H, phenyl protons), 7.13 (t, 1H, J 7.8, phenyl proton), 6.90 (d, 1H, J 7.8, phenyl proton), 5.98 (s, 1H, –CH=), 3.84 (br. t, 2H, J 7.2, NCH_2), 1.80 (br. s, 8H, $2CH_3$ and CH_2), 1.69–1.20 (m, 16H, CH_2), 0.88 (t, 3H, J 6.9, CH_3).

Anal. Calcd. for $C_{28}H_{34}N_5Cl$: C, 70.64; H, 7.20; N, 14.71. Found: C, 70.39; H, 7.30; N, 15.01.

3.1.3. 2-Chloro-5,6-dicyano-3-[2′-(1′-n-*hexadecyl-3′,3′-dimehylindolinylidene)-methyl]pyrazine (**3d**)*

Red crystals (57% yield) ir: ν CN 2218 cm^{-1}; ms: m/z 547 ([M+2]$^+$), 545 (M$^+$); ^{1}H NMR

($CDCl_3$): δ 7.30–7.25 ((t + d), 2H, phenyl protons), 7.13 (t, 1H, J 7.8, phenyl proton), 6.88 (d, 1H, J 7.8, phenyl proton), 5.90 (s, 1H, –CH=), 3.86 (br. t, 2H, J 7.2, NCH_2), 1.80 (br. s, 8H, $2CH_3$ and CH_2), 1.72–1.25 (m, 26H, CH_2), 0.88 (t, 3H, J 6.9, CH_3).

Anal. Calcd. for $C_{33}H_{44}N_5Cl$: C, 72.57; H, 8.12; N, 12.82. Found: C, 72.60; H, 8.20; N, 12.52.

*3.1.4. 2-Chloro-5,6-dicyano-3-[2′-(1′-*n*-nonylquinolinylidene)methyl]pyrazine (**4b**)*

Brown crystals (34% yield) ir: ν CN 2215 cm^{-1}; ms: m/z 433($[M+2]^+$), 431 (M^+); ^1H NMR ($CDCl_3$): δ 9.06 (d, 1H, J 9.6, phenyl protons), 7.74 (d, 1H, J 9.6, phenyl proton), 7.68 ((t + d), 2H, phenyl proton), 7.54 (d, 1H, J 8.7, phenyl protons), 7.39 (t, 1H, J 8.7, phenyl proton), 6.00 (s, 1H, –CH=), 4.28 (br. t, 2H, NCH_2), 1.99 (m, 2H, CH_2), 1.63(m, 2H, CH_2), 1.49 (m, 2H, CH_2), 1.30 (br. s, 8H, CH_2), 0.90 (t, 3H, J 6.9, CH_3).

Anal. Calcd. for $C_{25}H_{26}N_5Cl$: C, 69.51; H, 6.07; N, 16.21. Found: C, 69.68; H, 6.01; N, 15.94.

*3.1.5. 2-Chloro-5,6-dicyano-3-[4′-(1′-*n*-nonylquinolinylidene)methyl]pyrazine (**5b**)*

Blue crystals (28% yield) ir: ν CN 2220 cm^{-1}; ms: m/z 433($[M+2]^+$), 431 (M^+); ^1H NMR ($CDCl_3$): δ 8.54 (d, 1H, J 7.2, phenyl protons), 8.24 (d, 1H, J 7.2, phenyl proton), 7.76 (t , 1H, J 8.1, phenyl proton), 7.53 (m, 3H, phenyl protons), 6.76 (s, 1H, –CH=), 4.25 (br. t, 2H, NCH_2), 1.94 (m, 2H, CH_2), 1.27 (m, 12H, CH_2), 0.88 (t, 3H, J 6.9, CH_3).

Anal. Calcd. for $C_{25}H_{26}N_5Cl$: C, 69.51; H, 6.07; N, 16.21. Found: C, 69.40; H, 6.23; N, 16.28.

*3.1.6. 2-Chloro-5,6-dicyano-3-[4′-(1′-*n*-hexadecylquinolinylidene)methyl]pyrazine (**5c**)*

Blue crystals (34% yield) ir: ν CN 2222 cm^{-1}; ms: m/z 531 ($[M+2]^+$), 529 (M^+); ^1H NMR ($CDCl_3$): δ 8.60 (d, 1H, J 7.2, phenyl protons), 8.28 (d, 1H, J 7.2, phenyl proton), 7.75 (t, 1H, J 8.1, phenyl proton), 7.54 (m, 3H, phenyl protons), 6.81 (s, 1H, –CH=), 4.24 (t, 2H, NCH_2), 1.91 (m, 2H, CH_2), 1.25 (m, 26H, CH_2), 0.88 (t, 3H, J 6.9, CH_3).

Anal. Calcd. for $C_{32}H_{40}N_5Cl$: C, 72.50; H, 7.61; N, 13.21. Found: C, 72.31; H, 7.55; N, 13.09.

*3.2. Syntheses of **6** and **7***

To a solution of **3** (2.0 mmoles) in *N*,*N*-dimethylformamide (10 ml) was added dropwise 1.2-bis(2-aminoethoxy)ethane (10 mmoles), and the mixture was then stirred at 40∼45°C until all of **3** disappeared (tlc). The reaction mixture was poured into water (70 ml), the precipitate filtered, washed with water and dried. The compounds were recrystallized from ethylacetate.

*3.2.1. 1,2-Bis{2-[5′,6′-dicyano-3′-[2″-(1″,3″,3″-trimethylinolinylidene)methyl]-2′-pyrazinyl]aminoethoxy}ethane (**6a**)*

Yellow crystals (51% yield) ir: ν CN 2226 cm^{-1}; ^1H NMR (DMSO-d_6): δ 8.07 (br. s, 2H, NH), 7.26 (d, 2H, J 7.2, phenyl protons), 7.17 (t, 2H, J 7.2, phenyl proton), 6.93 (m, 4H, phenyl proton), 5.37 (s, 2H, –CH=), 3.54 (br. s, 12H, NCH_2 and OCH_2), 3.33 and 3.11 (s, 6H, NCH_3), 1.62 and 1.37 (s, 12H, CH_3).

Anal. Calcd. for $C_{42}H_{42}N_{12}2O_2$: C, 67.54; H, 5.67; N, 22.51. Found: C, 67.49; H, 5.54; N, 22.09.

*3.2.2. 1.2-Bis{2-[5′,6′-dicyano-3′-[2″-(1″-undecyl-3″,3″-dimethylindolinylidene)methyl]-2′-pyrazinyl]-aminoethoxy}ethane (**6b**)*

Yellow crystals (55% yield) ir: ν CN 2226 cm^{-1}; ^1H NMR (DMSO-d_6): δ 8.02 (br. s, 2H, NH), 7.26 (d, 2H, J 7.2, phenyl protons), 7.15 (t, 2H, J 7.5, phenyl proton), 6.92 (m, 4H, phenyl proton), 5.55 and 5.47 (s, 2H, –CH=), 4.07 and 3.96 (br. t, 4H, NCH_2), 3.51 (br. s, 12H, NCH_2 and OCH_2), 1.65 and 1.37 (s, 12H, CH_3), 1.57 (br. m, 4H, CH_2), 1.22∼0.99 (br. m, 32H, CH_2), 0.75 (t, 6H, J 7.2, CH_3).

Anal. Calcd. for $C_{62}H_{82}N_{12}O_2$: C, 72.48; H, 8.04; N, 16.36. Found: C, 72.74; H, 8.00; N, 16.35.

*3.2.3. 1.2-Bis{2-[5′,6′-dicyano-3′-[4″-(1″-*n*-hexadecylquinolinylidene)methyl]-2'-pyrazinyl] aminoethoxy}ethane (**7**)*

Blue crystals (69% yield) ir: ν CN 2217 cm^{-1}; ^1H NMR (DMSO-d_6): δ 8.42 (d, 2H, J 8.1, phenyl protons), 8.24 (d, 2H, J 8.1, phenyl protons), 7.96 (br. s, 2H, NH), 7.65 (m, 6H, phenyl proton), 7.32 (m, 2H, phenyl proton), 6.18 (s, 2H, –CH=), 4.11 (br. t, 4H, NCH_2), 3.56 (br. s, 12H, NCH_2 and OCH_2), 1.68–1.15 (br. m, 59H, CH_2), 0.80 (t, 6H, J 7.2,

CH_3). Anal. Calcd. for $C_{70}H_{94}N_5O_2$: C, 74.04; H, 8.34; N, 14.80. Found: C, 73.60; H, 8.38; N, 14.66.

References

[1] Levinson GS, Simpson WT, Curtius W. Journal of American Chemical Society 1957;79:4314.
[2] McRae EG, Kasha M. Journal of Chemical Physics 1958;28:721.
[3] Briggs JS, Herzenberg A. Molecular Physics 1971;21:8 65.
[4] Jaung JY, Matsuoka M, Fukunishi K. Dyes and Pigments 1998;37:135.
[5] Kim JH, Matsuoka M, Fukunishi K. Dyes and Pigments 1996;31:263.
[6] Matsuoka M. New synthesis of dicyanopyrazine related functional dyes: Functionalities and molecular stacking, in Griffiths J, Towns AD (eds), Colour science, 98, Vol. 2. Dyes and Pigment Chemistry, 1998.